C. R. Chimie 13 (2010) 661–667

Contents lists available at ScienceDirect

Comptes Rendus Chimie

www.sciencedirect.com

Full paper/Mémoire

Cu–Ln complexes with a single μ-oximato bridge

Jean-Pierre Costes [a,b,*], Laure Vendier [a,b]

[a] Laboratoire de chimie de coordination (LCC), CNRS, 205, route de Narbonne, 31077 Toulouse, France
[b] UPS, INPT, LCC, université de Toulouse, 31077 Toulouse, France

ARTICLE INFO

Article history:
Received 24 November 2009
Accepted after revision 10 March 2010
Available online 5 May 2010

Keywords:
Lanthanide
Copper
3d-4f complexes
Structural determinations
Magnetic properties

ABSTRACT

Two original dinuclear (Ln=Yb, **3** and Ln=Er, **4**) and one trinuclear Cu^{II}–Ln^{III}–Cu^{II} (Ln=Gd, 5) complexes derived from a polydentate non symmetrical Schiff base ligand H_2L have been prepared. The ligand possesses two functions (phenol and oxime) able to coordinate the Ln ions, but structural studies (X-ray diffraction and powder X-ray diffraction) show that the Cu^{II} and Ln^{III} ions are only bridged by the oximato (N–O) pair. The missing phenoxo bridge is replaced by a surprising pseudo-bridge involving one oxygen atom of the nitrato anion linked to the Cu and Ln ions according to a η^2: η^1: μ mode. Although this latter contact has no role from the magnetic point of view, it introduces a large deformation of the unique bridging network. The Cu–Yb complex **3** and the trinuclear Cu–Gd–Cu complex **5** present antiferromagnetic interactions, with a J_{CuGd} interaction equal to $-1.25\ cm^{-1}$ in **5**. The genuine single bridge can be considered as responsible for the antiferromagnetic character of the interaction.

© 2010 Académie des sciences. Published by Elsevier Masson SAS. All rights reserved.

1. Introduction

Ferromagnetic interactions between copper(II) and gadolinium(III) ions have been evidenced in a large majority of heterodinuclear Cu–Gd complexes published until now [1–3]. While the mechanism of ferromagnetic coupling was first suggested by D. Gatteschi [4] and then O. Kahn, [5] an interesting theoretical work has brought some advancement in the understanding of this phenomenon [6]. In conclusion of their work, these authors claimed that the large occurrence of approximate pseudo-C_{2v} geometry of Cu–Gd complexes could explain the generality of Cu–Gd ferromagnetic coupling. It becomes clear that the syntheses of di- or trinuclear complexes possessing different bridging networks should give supplementary information for the understanding of the active mechanism. Since then, a complex of lower symmetry with a phenoxo-hydroxo double bridge confirmed that a ferromagnetic interaction is still present [7]. Density functional studies on the exchange interaction of a dinuclear Cu–Gd complex published very recently suggest that the partially occupied Gd^{III} 5d orbitals have a major role on the magnetic coupling [8]. In the present work, we want to describe new complexes characterized by an original bridging network. Instead of having the classical double phenoxo bridge, these complexes do possess a single oximato bridge linking the copper and gadolinium ions. We describe the syntheses and structural determinations of two Cu–Ln complexes (Ln=Er, Yb), along with the magnetic studies of Cu–Gd complexes built with the same mononuclear copper complex.

2. Experimental section

2.1. Syntheses

The $Cu(Sal)_2$, [9] $Gd(hfa)_3{\cdot}2H_2O$ [10] complexes were obtained as previously described, as the ligand 1-(2,4,4-trimethyl-2-imidazolidinyl)-1-ethanone oxime resulting from the reaction of butanedione monoxime with 2-methyl-1,2-diaminopropane in a 1/1 ratio in diethyl ether [11]. As the different complexes are obtained with the

* Corresponding author.
E-mail address: jean-pierre.costes@lcc-toulouse.fr (J.-P. Costes).

1631-0748/$ – see front matter © 2010 Académie des sciences. Published by Elsevier Masson SAS. All rights reserved.
doi:10.1016/j.crci.2010.03.006

same experimental procedure, we will only describe a mononuclear precursor LCu·H_2O and a 3d-4f complex while analytical results and yields will be reported in each case.

LCu (1). A mixture of $Cu(Sal)_2$ (0.61 g, 1×10^{-3} mol), 1-(2,4,4-trimethyl-2-imidazolidinyl)-1-ethanone oxime (0.34 g, 2×10^{-3} mol) and triethylamine (0.2 g, 2×10^{-3} mol) in methanol (20 mL) was heated for twenty minutes, giving a violet solution, left to cool with stirring and filtered off. Addition of an equal amount of diethyl ether to the filtrate yielded a black precipitate, which was filtered off, washed with diethyl ether and air dried. Yield: 0.45 g (65%). Anal. Calcd for $C_{15}H_{19}CuN_3O_2$: (336.88) C, 53.5; H, 5.7; N, 12.5. Found: C, 53.2; H, 5.5; N, 12.3. IR (ATR): 2912m, 1635s, 1612s, 1594s, 1537m, 1465m, 1441s, 1415m, 1388m, 1375m, 1329m, 1300m, 1277s, 1246w, 1184m, 1158m, 1144m, 1124w, 1035w, 1005m, 916w, 891w, 761s, 737m, 692m cm^{-1}.

LNi·H_2O (2). Use of $Ni(Sal)_2{\cdot}2H_2O$ instead of $Cu(Sal)_2$ yielded the equivalent LNi complex that precipitated from the methanol solution as an orange solid. Yield: 0.5 g (75%). Anal. Calcd for $C_{15}H_{21}N_3NiO_3$: (350.04) C, 51.5; H, 6.0; N, 12.0. Found: C, 51.0; H, 5.8; N, 11.8. IR (ATR): 3357m, 2964w, 1630s, 1604m, 1530m, 1446s, 1400w, 1386m, 1353m, 1319m, 1306m, 1291s, 1170m, 1147m, 1128w, 1029w, 951w, 919w, 889w, 754m, 737m, 613w cm^{-1}.

[LCuYb(NO_3)$_3$(H_2O)$_2$]C_3H_6O (3). A mixture of LCu (0.10 g, 3×10^{-4} mol) and $Yb(NO_3)_3{\cdot}5H_2O$ (0.15 g, 3.2×10^{-4} mol) in acetone (10 mL) was heated for 10 mins and then left to cool with stirring and filtered off. Slow evaporation yielded crystals suitable for XRD. Yield: 0.17 g (71%). Anal. Calcd for $C_{18}H_{29}CuN_6O_{14}Yb$: (790.05) C, 27.4; H, 3.7; N, 10.6. Found: C, 27.2; H, 3.6; N, 10.2. IR (ATR): 3410m, 2978w, 1683m, 1630s, 1602m, 1548w, 1446s, 1335s, 1283s, 1215w, 1127m, 1029w, 914w, 814w, 766m, 743w, 698w cm^{-1}.

[LCuEr(NO_3)$_3$(H_2O)$_2$]C_3H_6O (4). Yield: (76%). Anal. Calcd for $C_{18}H_{29}CuErN_6O_{14}$: (784.27) C, 27.6; H, 3.7; N, 10.7. Found: C, 27.4; H, 3.5; N, 10.3. IR (ATR): 3421m, 2977w, 1682m, 1629s, 1602w, 1547w, 1459s, 1446s, 1334s, 1281s, 1216m, 1126m, 1028w, 914w, 814w, 766m, 741w, 697w cm^{-1}. Crystals were obtained by slow evaporation of an acetone solution.

($LCu)_2Gd(NO_3)_3{\cdot}H_2O$ (5). Yield: (85%). Anal. Calcd for $C_{30}H_{40}Cu_2GdN_9O_{14}$: (1035.04) C, 34.8; H, 3.9; N, 12.2. Found: C, 34.4; H, 3.6; N, 11.6. IR (ATR): 3150l, 2973w, 1632s, 1603m, 1543w, 1470s, 1445s, 1299s, 1279s, 1218m, 1190w, 1129s, 1027w, 915w, 816w, 764m, 742w, 695w cm^{-1}. We could not succeed in obtaining crystals suitable for XRD.

LCuGd(hfa)$_3$ (6). A mixture of LCu (0.034 g, 1×10^{-4} mol) and $Gd(hfa)_3{\cdot}2H_2O$ (0.082 g, 1×10^{-4} mol) in dichloromethane (10 mL) was heated for ten minutes, left to cool with stirring and filtered off. Slow evaporation yielded a black powder that was filtered off and air dried. Yield: 0.08 g (72%). Anal. Calcd for $C_{30}H_{22}CuF_{18}GdN_3O_8$: (1115.29) C, 32.3; H, 2.0; N, 3.8. Found: C, 32.5; H, 2.1; N, 4.0. IR (ATR): 2975w, 1655m, 1633m, 1608w, 1542m, 1525m, 1446m, 1249s, 1188s, 1130s, 791m, 756w, 659m cm^{-1}.

LNiYb(NO_3)$_3$(CH_3OH)(C_3H_6O) (7). A mixture of LNi·H_2O (0.11 g, 3×10^{-4} mol) and $Yb(NO_3)_3{\cdot}5H_2O$ (0.15 g, 3.2×10^{-4} mol) in a 1/1 acetone-methanol mixture (10 mL) was heated for ten minutes and then left to cool with stirring, yielding a yellow precipitate that was filtered off, washed with acetone, diethyl ether and air dried. Yield: 0.08 g (37%). Anal. Calcd for $C_{19}H_{29}N_6NiO_{13}Yb$: (781.21) C, 29.2; H, 3.7; N, 10.8. Found: C, 29.5; H, 3.5; N, 10.9. IR (ATR): 3340l, 2974w, 1633m, 1604m, 1479s, 1310s, 1254m, 1143m, 1032m, 765m, 713w, 679w, 611w cm^{-1}.

2.2. Materials and methods

All starting materials were purchased from Aldrich and were used without further purification. Elemental analyses were carried out by the *service de microanalyse du laboratoire de chimie de coordination*, Toulouse (C, H, N). Magnetic data were obtained with a Quantum Design MPMS SQUID susceptometer. The powder X-ray diffraction pattern was collected on a XPert Pro (Theta-Theta mode) Panalytical diffractometer with λ(Cu $K_{\alpha1}$, $K_{\alpha2}$) = 1.54059, 1.54439 Å. Magnetic susceptibility measurements were performed in the 2-300 K temperature range in a 0.1 T applied magnetic field, and diamagnetic corrections were applied by using Pascal's constants [12]. Isothermal magnetization measurements were performed up to 5 T at 2 K. The magnetic susceptibilities have been computed by exact calculations of the energy levels associated to the spin Hamiltonian through diagonalization of the full matrix with a general program for axial symmetry, [13] and with the MAGPACK program package [14] in the case of magnetization. Least-squares fittings were accomplished with an adapted version of the function-minimization program MINUIT [15].

2.2.1. Crystallographic data collection and structure determination for (3) and (4)

Crystals of **3** and **4** were kept in the mother liquor until they were dipped into oil. The chosen crystals were mounted on a Mitegen micromount and quickly cooled down to 180 K. The selected crystals of **3** (black, $0.25 \times 0.13 \times 0.06$ mm^3), **4** (pink, $0.3 \times 0.1625 \times 0.05$ mm^3) were mounted on a Stoe Imaging Plate Diffractometer System (IPDS) (**3**) or an Oxford-Diffraction XCALIBUR (**4**) using a graphite monochromator (λ = 0.71073 Å) and equipped with an Oxford Cryosystems cooler device. The data were collected at 180 K (**3**, **4**). The unit cell determination and data integration were carried out using the CrysAlis RED package for the data recorded on the Xcalibur and the Xred package for the STOE [16,17]. 12,237 reflections were collected for **3**, of which 4470 were independent (Rint = 0.0973), 9836 reflections for **4**, of which 5253 were independent (Rint = 0.02). The structures have been solved by Direct Methods using SIR92 [18], and refined by means of least-squares procedures on a F^2 with the aid of the program SHELXL97 [19] included in the softwares package WinGX version 1.63 [20]. The Atomic Scattering Factors were taken from International tables for X-Ray Crystallography [21]. All hydrogens atoms were geometrically placed and refined by using a riding model. All non-hydrogen atoms were anisotropically refined, and in the last cycles of refinement a weighting scheme was used, where weights are calculated from the following formula: $w = 1/[\sigma^2(Fo^2) + (aP)^2 + bP]$ where $P = (Fo^2 + 2Fc^2)/3$. Drawings

of molecules are performed with the program ORTEP32 [22] with 30% probability displacement ellipsoids for non-hydrogen atoms. CCDC 755654 and 755655 contain the supplementary crystallographic data for this paper. These data can be obtained free of charge at www.ccdc.cam.ac.uk/conts/retrieving.html or from Cambridge Crystallographic Data Centre, 12 Union Road, Cambridge CB2 1EZ, UK [Fax: Internat. +44-1223/336-033; email: deposit@ccdc.cam.ac.uk].

3. Results and discussion

The synthetic route to monomeric complexes **1** and **2** consists in reacting the corresponding salicylaldehyde metal complex with the half-unit ligand 1-(2,4,4,-trimethyl-2-imidazolidinyl)-1-ethanone oxime previously described [11]. This ligand, which precipitates as a cyclic aminal, reacts under its open-chain form with the salicylaldehydato metal complex. Owing to the non-symmetrical nature of the diamine, two isomeric forms are expected. In fact, ring opening concerns the most crowded C–N bond of the aminal and only one isomer is present. These LM (M=Cu, Ni) complexes are isolated under their deprotonated oxime form, with the metal ion surrounded by a (N_3O) chromophore and the oxygen oxime atom available for further coordination to a lanthanide ion. The formulations of the complexes resulting from reaction with lanthanide salts are deduced from analytical data. They vary all along the lanthanide series, giving [LCuLn$(NO_3)_3(H_2O)_2$] complexes with heavier Ln ions (Er **4**, Yb **3**) and a trinuclear $(LCu)_2Gd(NO_3)_3(H_2O)$ **5** complex with gadolinium. Nevertheless, a 1/1 Cu/Gd **6** complex is isolated by reacting LCu with $Gd(hfa)_3{\cdot}2H_2O$. We will see later that the equivalent nickel complexes are of a lesser interest, so that only the Ni–Yb **7** complex has been prepared.

3.1. Structural studies of [LCuYb$(NO_3)_3(H_2O)_2$] 3 and [LCuEr$(NO_3)_3(H_2O)_2$] 4

The crystallographic data of complexes **3** and **4** are summarized in Table 1 while views of both structures are reported in Figs. 1 and 2, respectively. Relevant bond distances and angles are collated in the figure captions. The two isostructural structures crystallize in the triclinic P-1 space group. We previously reported Cu–Ln complexes made with ligands having phenol and oxime functions, but also a methoxy group in the α position of the phenol functions creating a O_3 coordination site for the Ln ion [23]. In the present work, the mononuclear copper complex used to make Cu–Ln entities possesses an outer coordination site reduced to the oxygen atoms of the oxime and phenol functions. The structural determinations do confirm that the Cu and Ln ions are only linked by a single oxime N–O bridge, the phenoxo oxygen atom not being involved in coordination with the Ln ion. At first view, the missing phenoxo bridge is replaced by a surprising pseudo-bridge involving one oxygen atom of the nitrato anion linked to the Cu and Ln ions according to a η^2: η^1: μ mode. But the copper ion in **3** and **4** cannot be considered in a square-pyramidal environment with this axial nitrato oxygen atom and the four basal donor atoms O(13)N(4)N(5)N(6) of the ligand. Indeed, the Cu–O distance is large (2.783(4) and 2.758(3) Å in **3** and **4**, respectively) and it seems more correct to speak about a weak pseudo-contact. This is corroborated by the presence of the copper ion in the mean coordination plane of the

Table 1
Crystallographic Data for [LCuYb$(NO_3)_3(H_2O)_2]C_3H_6O$ **3** and [LCuEr$(NO_3)_3(H_2O)_2]C_3H_6O$ **4**.

	3	**4**
Chem formula	$C_{18}H_{29}CuN_6O_{14}Yb$	$C_{18}H_{29}CuErN_6O_{14}$
Fw	789.04	784.28
Space group	P-1 (No. 2)	P-1 (No. 2)
a, Å	10.5307(12)	10.554(5)
b, Å	11.4551(12)	11.484(5)
c, Å	11.5227(12)	11.547(5)
α, deg	86.845(13)	86.877(5)
β, deg	85.073(13)	85.085(5)
δ, deg	89.636(13)	89.685(5)
V, Å^3	1382.7(3)	1392.3(11)
Z	2	2
ρ_{calcd}, g cm^{-3}	1.895	1.861
λ, Å	0.71073	0.71073
T, K	180	180
$\mu_{MoK\alpha}$, mm^{-1}	4.206	3.832
R[a] obs, all	0.0358, 0.0813	0.0209, 0.0497
Rw[b]obs, all	0.0427, 0.0837	0.0226, 0.0404

[a] $R = \Sigma||Fo|-|Fc||/\Sigma|Fo|$. [b] $wR = [\Sigma w(|Fo^2|-|Fc^2|)^2/\Sigma w|Fo^2|^2]^{1/2}$.

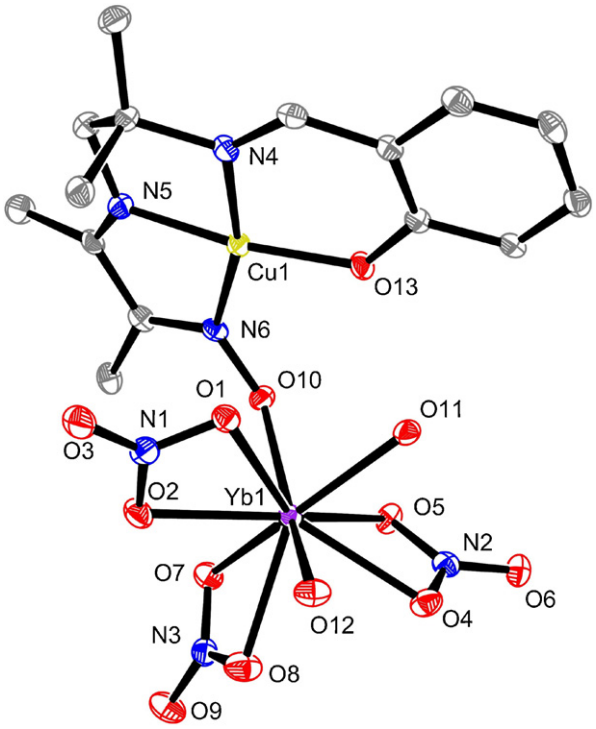

Fig. 1. Molecular plot for **3** with ellipsoids drawn at the 30% probability level. Selected bond lengths (Å) and angles (°): Cu1-N4 1.952(5), Cu1-N5 1.936(5), Cu1-N6 2.006(5), Cu1-O13 1.889(4), Cu1-O1 2.758(4), N6-O10 1.333(6), Yb1-O1 2.448(4), Yb1-O2 2.388(4), Yb1-O4 2.451(4), Yb1-O5 2.442(4), Yb1-O7 2.430(4), Yb1-O8 2.416(4), Yb1-O10 2.173(4), Yb1-O11 2.268(2), Yb1-O12 2.322(4), O10-N6-Cu1 126.8(3), N6-O10-Yb1 128.0(3)°.

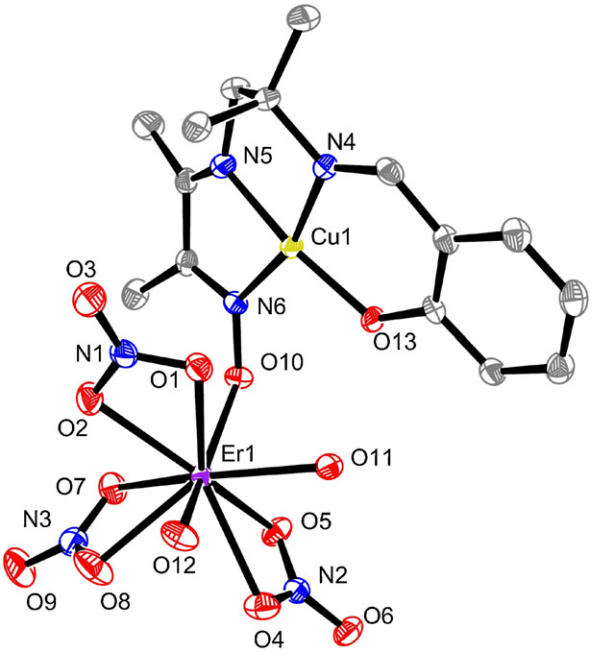

Fig. 2. Molecular plot for **4** with ellipsoids drawn at the 30% probability level. Selected bond lengths (Å) and angles (°): Cu1-N4 1.949(2), Cu1-N5 1.934(2), Cu1-N6 2.000(2), Cu1-O13 1.890(2), Cu1-O1 2.783(2), N6-O10 1.339(3), Er1-O1 2.458(2), Er1-O2 2.410(2), Er1-O4 2.469(2), Er1-O5 2.449(2), Er1-O7 2.449(2), Er1-O8 2.445(2), Er1-O10 2.202(2), Er1-O11 2.308(2), Er1-O12 2.346(2), O10-N6-Cu1 126.9(2), N6-O10-Er1 127.8(2)°.

deprotonated ligand. This Cu–O straight line makes an angle of 25.5(1) or 25.8(1)° to the normal of the mean basal plane in **3** and **4**. The imine nitrogen atom of the butanedione ligand deviates from the mean coordination plane by 0.112(4) Å in **3** and **4**. As a consequence, the oxygen atom of the oxime function deviates from this mean plane by 0.393(3) and 0.384(2) Å in **3** and **4**, on the opposite direction. Also, the five-membered ring formed by the diamine moiety chelating the copper ion is non planar, as usual, with a δ gauche conformation. The ytterbium and erbium ions are nonacoordinate in both complexes. They are surrounded by one oxygen atom of the oxime function O(10) from L, six oxygens from the three nitrato auxiliary ligands (two chelating and one chelating and bridging in a η^2: η^1: μ mode) and two oxygens from two water molecules.

In both complexes, the central part of the structure is occupied by the Cu^{II} and Ln^{III} ions connected by a single bridge involving the N–O oxime atoms on the one hand, and a pseudo-bridge sustained by the oxygen of a nitrato ligand. The bridging networks Cu(O, N–O)Gd are not planar and the role of the pseudo-contact is mainly limited to the increase of the N–O–Ln angle, 128.2(3) and 127.9(3)° for **3** and **4**, respectively. The dihedral angles between the planes (O(13)N(4)N(5)N(6)) and (O(1)LnO(3)) are equal to 67.2(1)° in **3** and 66.9(1)° in **4**. The intramolecular Cu...Ln separations vary from 4.238(1) Å in **3** to 4.263(1) Å in **4** and the shortest interunit metal contacts are: Cu...Cu = 5.720(2) Å, Yb...Yb = 7.149(1) Å in **3** and Cu...Cu = 5.734(2) Å, Er...Er = 7.184(1) Å in **4**.

As usual, the Ln–O bond lengths depend on the nature of the oxygen atoms. The shortest bond is the oximato Ln–O(10) bond (2.173(4) Å in **3** and 2.202(2) Å in **4**). The lengths of the Ln–O (nitrato) bonds vary from 2.388(4) Å to 2.451(4) Å in **3** and from 2.410(2) Å to 2.469(2) Å in **4**, thus reflecting the larger Lewis acidity of the Yb ion in comparison to the Er ion. The Ln–O(water) bond lengths follow the same tendency (from 2.268(2) and 2.322(4) Å in **3** to 2.308(2) and 2.346(2) Å in **4**).

In conclusion of the structural study, we can consider that the Cu–Ln complexes made with the starting copper complex used as a ligand and heavier Ln ions have similar geometric characteristics. As expected, the Cu–N and Cu–O bond lengths are quite identical in the two complexes while the Ln–O bond lengths are shorter from 0.02–0.03 Å in **3**, in agreement with the larger Lewis acidity of the Yb ion. On the contrary, we can notice the constancy of several geometrical parameters, such as the angles of the Cu–N–O–Ln bridges, the position of the oxygen oxime atom out of the mean copper coordination plane, the presence of a pseudo-bridge involving a nitrato ligand and absence of a phenoxo bridge.

3.2. Magnetic properties

We report in Fig. 3 the magnetic behavior of complex **4** in the form of the thermal variation of the $\chi_M T$ product (χ_M is the molar magnetic susceptibility corrected for the diamagnetism of the ligands) [12]. In the present case the $\chi_M T$ product, which is equal to 11.2 $cm^3mol^{-1}K$ at 300 K stays practically constant until to 100 K, decreases between 100 and 2 K, where it is equal to 4 $cm^3mol^{-1}K$. The $\chi_M T$ at room temperature is in the range of the expected value for isolated Cu and Er ($J = 15/2$, $g_J = 6/5$) ions (11.85 $cm^3mol^{-1}K$). For complex **3**, the $\chi_M T$ product, which is equal to 2.7 $cm^3mol^{-1}K$ at 300 K, is not far from the 2.94 $cm^3mol^{-1}K$ expected value for non interacting Cu and Yb ($J = 7/2$, $g_J = 8/7$) ions (Fig. 4, diamonds). On the contrary a monotonic decrease, from 2.25 $cm^3mol^{-1}K$ at 300 K to 1.27 $cm^3mol^{-1}K$ at 2 K, is observed for the Ni–Yb complex **7**, as indicated in Fig. 4 (circles). In the presence of orbital degeneracy, the exchange phenomenon is a difficult task, without any general solution for such complexes do not obey the Curie law, even in the absence of any exchange

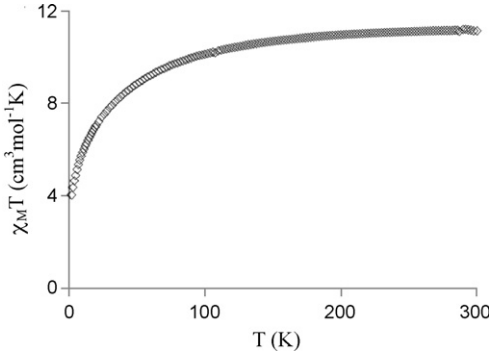

Fig. 3. Experimental $\chi_M T$ vs. T for $[LCuEr(NO_3)_3(H_2O)_2]C_3H_6O$ **4**.

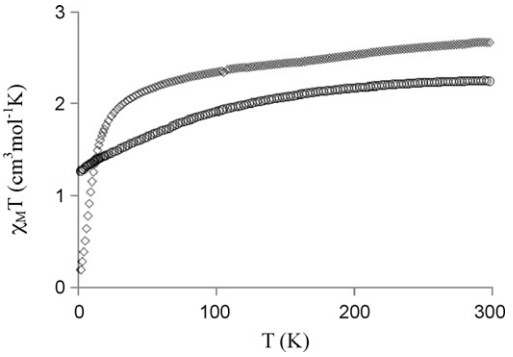

Fig. 4. Experimental $\chi_M T$ vs. T for $[LCuYb(NO_3)_3(H_2O)_2]C_3H_6O$ **3** (diamonds) and for $[LNiYb(NO_3)_3(CH_3OH)](C_3H_6O)$ **7** (circles).

interaction. In general, comparison of a Cu–Ln complex with its M–Ln analogue, where M is a diamagnetic ion, must give magnetic data devoid from the Ln orbital contribution, so that the difference curve furnishes a qualitative information on the nature of the active magnetic interaction [24,25]. This method has been applied to complexes Cu–Yb **3** and Ni–Yb **7**. If the difference curve gives the expected 0.4 $cm^3mol^{-1}K$ at high temperature, what corresponds to the $\chi_M T$ product of the copper ion, this curve diverges at lower temperatures to give negative values. An easy explanation can be put forward. In the $LNiYb(NO_3)_3(CH_3OH)(C_3H_6O)$ complex **7**, the diamagnetic nickel ion in a square planar environment prevents formation of a Ni–O–Ln η^2: η^1: μ nitrato pseudo-bridge, and induces by the way a change in the N–O–Yb angle of the oxime bridge and in the Yb coordination sphere. This structural change must introduce a variation in the Yb crystal field effects applied to the Cu–Yb and Ni–Yb complexes **3** and **7**. A variation in the energy distribution of the Stark sublevels is expected, so that the curve difference method, $\chi_M T(3) - \chi_M T(7)$ (Fig. 4), [24,25] that gives a qualitative information on the magnetic interaction, must be used with caution. Nevertheless, the very low $\chi_M T$ value (0.19 $cm^3mol^{-1}K$) observed at 2 K for complex **3** (Fig. 4, diamonds) allows to conclude that an antiferromagnetic Cu–Yb interaction is active in complex **3**.

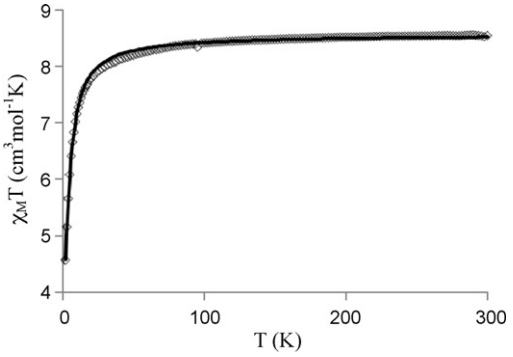

Fig. 5. Experimental $\chi_M T$ vs. T for $(LCu)_2Gd(NO_3)_3.H_2O$ **5**. The solid line corresponds to the best fit described in the text.

The temperature dependence of the magnetic susceptibilities for complexes **5** and **6** in the 2–300 K temperature range is shown in Figs. 5 and 7 in the $\chi_M T$ vs. T form. At 300 K, $\chi_M T$ is equal to 8.54 $cm^3mol^{-1}K$ which nicely corresponds to the value expected for the two copper and one gadolinium ($S = 7/2$, $g_J = 2$) uncoupled metal ions (8.62 $cm^3mol^{-1}K$). Lowering the temperature causes $\chi_M T$ to decrease slowly until 30 K (8.0 $cm^3mol^{-1}K$) and then more abruptly to 4.57 $cm^3mol^{-1}K$. The experimental data indicate the occurrence of an overall antiferromagnetic interaction in complex **5**. Finally, fitting the experimental data to a simple model derived from the spin only Hamiltonian for a trinuclear (Cu–Gd–Cu) complex, $H = -J_{CuGd}(S_{Cu1}.S_{Gd} + s_{Cu2}.S_{Gd})$ yields the following data, $J_{CuGd} = -1.25\ cm^{-1}$, $g = 1.99$ with an R factor equal to $3.0\ 10^{-5}$, $R = \Sigma[(\chi_M T)^{obs} - (\chi_M T)^{calc}]^2/\Sigma[(\chi_M T)^{obs}]^2$. As the Cu ions are well separated from each other, without any direct link, a Cu–Cu interaction is not taken into consideration in the above Hamiltonian. A similar behavior is observed for complex **6** (Fig. 7). Use of an isotropic Hamiltonian for a dinuclear (Cu–Gd) complex, $H = -J_{CuGd}(S_{Cu}.S_{Gd})$ gives $J_{CuGd} = -0.76\ cm^{-1}$, $g = 2.04$ and $R = 1.0\ 10^{-4}$. In these two complexes, the antiferromagnetic Cu–Gd interactions are confirmed by the field dependence of magnetization M at 2 K. These experimental values are correctly fitted with the Brillouin functions corresponding to $S = 5/2$ (complex **5**, Fig. 6) and to $S = 3$ (complex **6**, Fig. 8) spin states. The magnetization curve for complex **5** is clearly located below the theoretical curve (dashed line in Fig. 6) corresponding to a trinuclear Cu–Gd–Cu complex in which the copper and gadolinium do not interact (Figs. 7 and 8).

4. Discussion

The heavier lanthanide nitrate salts do react with the non symmetrical Schiff base complex LCu acting as a ligand to yield heterodinuclear $LCuLn(NO_3)_3(H_2O)_2$ entities (Ln=Er, Yb) in which the metal ions are bridged by an unique oxime bridge. It has been found in many Cu–Ln complexes that the copper ion adopts a square-based 4 + 1 coordination mode [9]. This weak axial coordination is very often held by solvent molecules (acetone, methanol). In the present structures, the weak contact

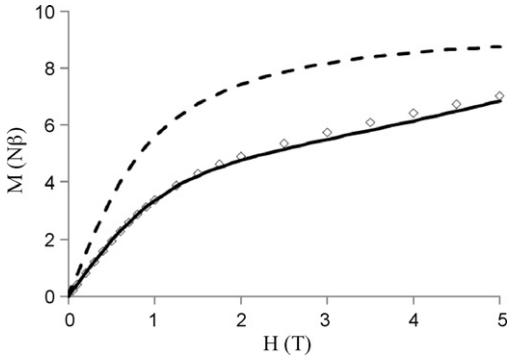

Fig. 6. Field dependence of the magnetization for $(LCu)_2Gd(NO_3)_3.H_2O$ **5** at 2 K. The solid line corresponds to the best fit described in the text and the dashed line to the Brillouin function for non-interacting ions.

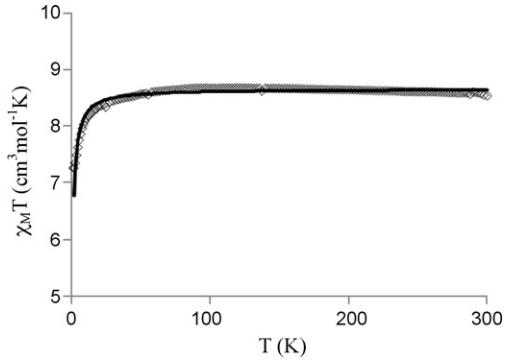

Fig. 7. Experimental $\chi_M T$ vs. T for LCuGd(hfa)$_3$ **6**. The solid line corresponds to the best fit described in the text.

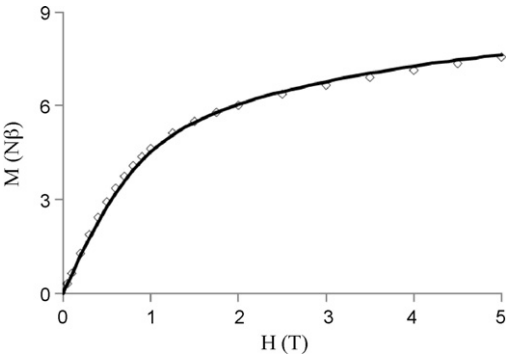

Fig. 8. Field dependence of the magnetization for LCuGd(hfa)$_3$ **6** at 2 K. The solid line corresponds to the best fit described in the text.

is established by one oxygen atom of a nitrato anion chelating the Ln ion, thus making an unexpected Cu–O–Ln η^2: η^1: μ nitrato pseudo-bridge [26]. This contact is responsible for the constancy of the geometrical parameters found in such complexes, the N–O–Ln angles (128.2(3) and 127.9(3)° for **3** and **4**, respectively) and the dihedral angles between the mean copper O(13)N(4)N(5)N(6) coordination plane and the O(1)LnO(10) plane (67.2(1)° in **3** and 66.9(1)° in **4**). From the magnetic point of view, this pseudo-bridge is out of importance for two mains reasons. Indeed, nitrato anions are known as being unable to support any significant magnetic coupling [27] and the d_{x2-y2} copper magnetic orbital lies orthogonal to the axial pseudo-bridge.

The use of gadolinium nitrate gives a trinuclear $(LCu)_2Gd(NO_3)_3{\cdot}H_2O$ complex that does not crystallize. At first sight, this complex seems to be similar to the trinuclear $(LCu)_2Ce(NO_3)_3$ complex previously published [28], but a comparative powder XRD study confirms that the structures of these two complexes are different (Figure S1). The $(LCu)_2Ce(NO_3)_3$ structure differs from the structures of complexes **3** and **4** by the LCu/Ln ratio, 2/1 instead of 1/1, and also by the coordination of the large cerium ion to the oxime and phenoxo oxygen atoms. On the contrary, the Cu–O–Ln η^2: η^1: μ nitrato pseudo-bridge is present in all cases, whatever the 2/1 or 1/1 LCu/Ln ratio. These data do confirm that the nitrato pseudo-bridges are still present in the $(LCu)_2Gd(NO_3)_3{\cdot}H_2O$ complex and that the gadolinium ion is only linked to the deprotonated oxime, as in complexes **3** and **4**. These conclusions do agree with a recent work in which the LCu or LNi complexes are used as ligands to build tetranuclear Cu–Mn–Mn–Cu and Ni–Mn–Mn–Ni complexes [29]. Again, the oxime bridges Cu–N–O–Mn or Ni–N–O–Mn are the only ones to link the metal ions. The N–O–Mn angles of the oxime function with the Mn ions vary from 117.5(2) to 118.7(2)°, not far from the angles found in the present Cu–Ln structures (128.0(3)°), thus confirming that large N–O–M angles are characteristic for such ligands. As expected, the Cu–N–O angles of the oxime function with the Cu ions are identical in the two sets of complexes (126.4(2)° against 126.9(2)° in our complexes).

Until now, it has been observed that the interaction parameter J for complexes with a CuO_2Gd core depends on the dihedral angle (OCuO, OGdO) between the planes involving each metal ion and the bridging oxygen atoms, the ferromagnetic interaction decreasing with an increase of the dihedral angle and becoming antiferromagnetic for large angles [30]. A comparison with the Cu–Gd complex made with a ligand similar to the one used in this work, having phenol and oxime functions and a supplementary methoxy group in the α position of the phenol function is quite informative [23]. Indeed, introducing a methoxy group creates a O_3 coordination site for the Ln ion that becomes then double-bridged to the copper ion by the oximato and phenoxo functions. From the magnetic point of view, this ligand change introduces a major difference in the magnetic interaction, which was ferromagnetic ($J = 3.5\ cm^{-1}$) or slightly antiferromagnetic with large dihedral angles in the previous example [23] and becomes antiferromagnetic ($J = -1.25\ cm^{-1}$) here in the trinuclear $(LCu)_2Gd(NO_3)_3{\cdot}H_2O$ complex **5**. We cannot speak about the dihedral angle in the complexes studied here, as we have a single bridge, but it becomes clear that the presence of a single bridge is the factor responsible for the interaction change, from ferro to antiferromagnetic. A replacement of nitrato anions by hexafluoroacetylacetonato ligands yields the dinuclear LCuGd(hfa)$_3$ complex **6** that possesses a weaker antiferromagnetic J interaction ($-0.76\ cm^{-1}$ instead of two interactions of $-1.25\ cm^{-1}$ in **5**). This weakening of J can be explained by a change in the N–O–Gd angle of the bridging oxime due to the disappearance of the nitrato pseudo-bridge, the oxygen atoms of the hfa ligands being unable to interact with the copper ion.

In a very recent work dealing with the Cu–Gd exchange interaction, DFT calculations demonstrate that replacement of one bridging oxygen by a hydrogen atom in a double bridge should give antiferromagnetic interactions [8]. In other words, this would mean that an unique bridge, as in the present complexes $(LCu)_2Gd(NO_3)_3{\cdot}H_2O$ **5** and LCuGd(hfa)$_3$ **6**, should yield antiferromagnetic interactions. This work gives an experimental support to these calculations, antiferromagnetic interactions being observed in complexes **5** and **6**.

5. Conclusion

We have shown in this work that a mononuclear complex derived from a non-symmetrical Schiff base ligand reacts with lanthanide nitrate salts to yield di or trinuclear Cu–Ln or Cu–Ln–Cu complexes, depending on the Lewis acidity or size of the Ln ions. These genuine complexes differ from previous Cu–Ln complexes for the Cu and Ln ions are bridged by a single and unique oximato bridge. The Ln ions are nine coordinate, linked to the deprotonated oxygen atom of the oxime function, six oxygen atoms coming from three chelating nitrato ligands, and two water molecules. One oxygen atom of a chelating nitrato ligand makes a pseudo-contact with the copper ion, introducing a weak axial contact (Cu. . .O larger than 2.75 Å) not able to attract the copper ion out of the mean N_3O coordination site of the ligand. The main function of this pseudo-contact consists in increasing the N–O–Ln angle to a constant value of 128.0(3)°. Contrary to the large majority of Cu–Gd complexes characterized by ferromagnetic Cu–Gd interactions, antiferromagnetic interactions are active in the trinuclear $(LCu)_2Gd(NO_3)_3{\cdot}H_2O$ complex. Replacement of the nitrato ligands surrounding the Gd ion by hexafluoroacetylacetonato ligands yields a dinuclear $LCuGd(hfa)_3$ complex, suppresses the Cu–O–Ln η^2: η^1: μ nitrato pseudo-bridge and introduces a change in the N–O–Gd angle that must be responsible for the decrease of the J_{Cu-Gd} interaction which is still antiferromagnetic. This antiferromagnetic behavior, which is also active in the corresponding Cu–Yb complex, is attributed to the presence of a unique oxime bridge in between the Cu and Gd ions. Such a behavior was previously observed in complexes possessing an outer O_3 coordination site for the Ln ion involving phenoxo and oximato oxygen atoms and a supplementary methoxy oxygen. In this latter case, the change from a ferro- to an antiferromagnetic interaction was attributed to the increase of the dihedral angle between the planes involving each metal ion and the bridging oxygen atoms. A comparison between these two data sets is at present beyond the scope of the present work.

Acknowledgements

This work was supported by the European Union sixth framework program NMP3-CT-2005-515767 entitled "*MAGMANet:* mol*ecular Approach to Nanomagnets and Multifunctional Materials*". The authors are grateful to Dr. A. Mari for technical assistance for the magnetic measurements.

Appendix A. Supplementary data

Supplementary data associated with this article can be found, in the online version, at doi:10.1016/j.crci.2010.03.006.

References

[1] C. Benelli, D. Gatteschi, Chem. Rev. 102 (2002) 2369.
[2] M. Sakamoto, K. Manseki, H. Okawa, Coord. Chem. Rev. 219–221 (2001) 379.
[3] M. Andruh, J.P. Costes, C. Diaz, S. Gao, Inorg. Chem. 48 (2009) 3342.
[4] C. Benelli, A. Caneschi, D. Gatteschi, O. Guillou, L. Pardi, Inorg. Chem. 29 (1990) 1750.
[5] O. Kahn, Magneto-Structural Correlations in Exchange Coupled Systems, in: R. D. Willet, D. Gatteschi, O. Kahn, (Eds.), D. Reidel, 1985.
[6] J. Paulovic, F. Cimpoesu, M. Ferbinteanu, K. Hirao, J. Am. Chem. Soc. 126 (2004) 3321.
[7] F.Z. Chiboub Fellah, J.P. Costes, F. Dahan, C. Duhayon, G. Novitchi, J.P. Tuchagues, L. Vendier, Inorg. Chem. 47 (2008) 6444.
[8] G. Rajaraman, F. Totti, A. Bencini, A. Caneschi, R. Sessoli, D. Gatteschi, Dalton Trans. (2009) 3153.
[9] J.P. Costes, F. Dahan, A. Dupuis, J.P. Laurent, Inorg. Chem. 36 (1997) 3429.
[10] M.F. Richardson, W.F. Wagner, D.E. Sands, J. Inorg. Nucl. Chem. 30 (1968) 1275.
[11] J.P. Costes, F. Dahan, A. Dupuis, J.P. Laurent, New J. Chem. (1998) 1525.
[12] P. Pascal, Ann. Chim. Phys. 19 (1910) 5.
[13] A.K. Boudalis, J.-M. Clemente-Juan, F. Dahan, J.-P. Tuchagues, Inorg. Chem. 43 (2004) 1574.
[14] (a) J.J. Borrás-Almenar, J.M. Clemente-Juan, E. Coronado, B.S. Tsukerblat, Inorg. Chem. 38 (1999) 6081 ;
(b) J.J. Borrás-Almenar, J.M. Clemente-Juan, E. Coronado, B.S. Tsukerblat, J. Comput. Chem. 22 (2001) 985.
[15] F. James, M. Roos, MINUIT Program, a System for Function Minimization and Analysis of the Parameters Errors and Correlations, Comput. Phys. Commun. 10 (1975) 345.
[16] CrysAlis RED, version 1.170.32; Oxford Diffraction Ltd., 2003.
[17] STOE: IPDS Manual, version 2.75; Stoe & Cie, Darmstadt, Germany, 1996.
[18] SIR92 - A program for crystal structure solution. A. Altomare, G. Cascarano, C. Giacovazzo, A. Guagliardi, J. Appl. Crystallogr. 26 (1993) 343.
[19] SHELX97 [Includes SHELXS97, SHELXL97, CIFTAB] - Programs for Crystal Structure Analysis (Release 97-2). G. M. Sheldrick, Institüt für Anorganische Chemie der Universität, Tammanstrasse 4, D-3400 Göttingen, Germany, 1998.
[20] WINGX - 1.63 Integrated System of Windows Programs for the Solution, Refinement and Analysis of Single Crystal X-Ray Diffraction Data. L. Farrugia, J. Appl. Crystallogr. 32 (1999) 837.
[21] International tables for X-Ray crystallography, Vol IV, Kynoch press, Birmingham, England, 1974.
[22] ORTEP3 for Windows - L. J. Farrugia, J. Appl. Crystallogr. 30 (1997) 565.
[23] J.P. Costes, F. Dahan, A. Dupuis, J.P. Laurent, Inorg. Chem. 39 (2000) 169.
[24] J.P. Costes, F. Dahan, A. Dupuis, J.P. Laurent, Chem. Eur. J. 4 (1998) 1616.
[25] M.L. Kahn, C. Mathonière, O. Kahn, Inorg. Chem. 38 (1999) 3692.
[26] L.W. Yang, S. Liu, S.J. Rettig, C. Orvig, Inorg. Chem. 34 (1995) 4921.
[27] H.M.J. Hendricks, P.J.M. Birker, J. van Rijn, G.C. Verschoor, J. Reedijk, J. Am. Chem. Soc. 104 (1982) 3607.
[28] J.P. Costes, F. Dahan, A. Dupuis, Inorg. Chem. 39 (2000) 5994.
[29] C. Kachi-Terajima, H. Miyasaka, A. Saitoh, N. Shirakawa, M. Yamashita, R. Clérac, Inorg. Chem. 46 (2007) 5861.
[30] J.P. Costes, F. Dahan, A. Dupuis, Inorg. Chem. 39 (2000) 165.